Digital representation of tissues in high compute bioelectromagnetics

Artur Krupa *, Izabella Antoniuk

Institute of Information Technology, Warsaw University of Life Sciences WULS-SGGW, Poland

ARTICLE INFO

ABSTRACT

Representing any type of living tissue in digital form is a complex and demanding problem due to its heterogeneous structure as well as different issues that can be encountered during such transition. Usually, to ensure faster computation times, models are simplified, i.e. by averaging available parameters. Such an approach can result in omitting essential features and, consequently, lead to lower accuracy of obtained results.

In simulations, bioelectromagnetism uses a different approach to numerical calculations. Additionally, models are used to represent the phenomena they describe. This article presents an approach to tissue representation in the field of bioelectromagnetic simulations and research, which is the result of work carried out by the authors in this field in recent years.

The description of the model is widely discussed in the paper, taking into account the problem of numerical uncertainty, reliability, averaging or the adopted geometry. Each concept is presented in the examples, along with the possible level of minimization of the impact on the simulation results. The work also includes an exemplary model with a parametric description of tissues and the impact of these problems on the actual results. We present an analysis showing which parameters are essential for tissue modelling, how the complexity of a model influences a simulation and how using different tissue models can impact the relation between total simulation time and output effectiveness. The simulation process was based on a large-scale cloud computing environment with the presented design, simulation and optimization solution, one of the many available.

Currently, methods described in this paper are not standardly incorporated in widely used solvers or simulations. Results presented can lead to unification and standardization of current tissue modelling methodologies, improving overall computation standards in research on the impact of electromagnetic field on living organisms.

1. Introduction

The problem of human tissue representation in digital form, used for simulations in mathematics, mechanics or electrical engineering, has been discussed in the scientific literature since the first half of the 20th century. At the same time, modelling problems with the use of computing machines at that time did not appear until the 1960s. In the beginning, the central theme of the described research was the transfer of the biological state to a mathematical notation that would allow the definition of individual organs, unified tissues or even entire objects constituting a simulation model of the human body. Thanks to an increasingly detailed understanding of anatomy as well as more complex mathematical

functions and technological development, the quality of the simulations, models and their digital representation have improved significantly.

One of the first similarly described works, when it comes to the subject of tissue modelling, is [1]. In this case, the numerical model for the capillary–tissue system was defined, which is responsible for oxygen transportation in cerebral grey matter. The presented definition assumes significant simplifications in overall representation instead of focusing on defining the problem in a controlled way and propose, above all, an understanding of the functioning of the biological oxygen transport system. Another example, which uses the mathematical model, uses the finite element method to visualize the mesh describing human aortic valve leaflets [2]. A completely different yet also numerical approach is described in [3]. The authors present the reconstruction of the mathematical model of the human chest on the basis of the potential from the electrodes using the inverse solution.

The works mentioned here, as well as many others published in later years (like [4,5]), show how complex the problem of tissue representation in computer simulations can be. There are many issues that need to be considered throughout the entire process, starting with mathematical model recording and finishing with its digital representation. What is often done in order to decrease the overall model complexity is simplifying the model parameters. This allows for faster processing of the research scenario and results based on the created model, but in turn, it can lead to outcomes that are far from reality. This problem is mainly connected to the significant variability and diversity of tissues. It is assumed in this work that human tissues are considered, and an impact of different medical, technological or physical research has on man in the general and human body specifically.

This paper presents the results of recent research performed by the authors of [6,7] on the problem of tissue structure complexity. The process of model parameters selection is discussed and outlined. In addition, the example object model, along with its mathematical definition and obtained simulation results, will be discussed based on the chosen scenario. For performed research, both numerical results obtained from the complex, dedicated computer system and environment functioning description will be presented.

2. Model definition

Research conducted in recent years on tissue modelling confirmed how complex a realistic human model is [8–10]. The models used in simulations are usually either averaged, statistical objects or they are significantly simplified. Both approaches limit the reliability of the results. The research cases discussed and analysed in this work will mainly concern the broadly understood concept of bioelectromagnetism used in medicine in applications such as:

- Threads
- Therapy
- Diagnosis

The significant research which uses simulations based on tissue models, as well as partial and comprehensive models of the human body, the following examples can be mentioned:

- Magnetic Resonance Imaging (MRI)
- Electric Muscle Stimulation (EMS)
- Electroconvulsive Therapy (ECT)
- Environmental Magnetic Field (EMF)

For the purpose of the analysis presented in this work, the considered studies were limited to the scenarios which are related to the impact of the electromagnetic field on the human body and selected tissues. This topic was chosen due to the increasing importance of developing technology impact on the human body and increasingly restrictive safety standards. Especially the influence of low frequencies was considered since they ensure greater propagation of the electromagnetic wave into the tissues.
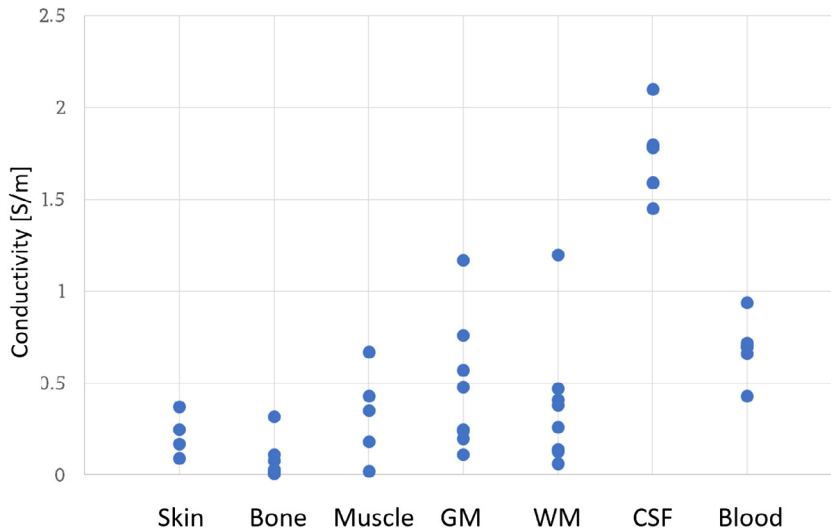
2.1. Uncertainty problem

The knowledge developed and gained in the course of the work showed that from the point of view of the concept of tissue modelling, both their geometry as well as input and output parameters, which are the basis of a given simulation scenario, are important. However, when introducing the model to the calculations, the concept of Uncertainty Quantification (UQ) appears. By definition, it is uncertainty regarding the parameters that can be used to describe a given model — including the source affecting this uncertainty, the scale and the possibility of its reduction. Table 1 presents the four primary sources of uncertainty in tissue modelling, along with their averaged level of constraints.

The primary division criterion is the type of constraints that may be related to the lack of knowledge - *epistemic* uncertainty or to statistical variability - *aleatoric* uncertainty. The first type is usually the lack of sufficient knowledge or experience, which can be reduced by improving the accuracy of the test method or rounding. In other words, this limitation can be removed or almost entirely reduced by improving R&D accuracy. The second type is a set of constraints related to inherent variations, which are defined in parametric accuracy and, in general, cannot be reduced. In this case, the appropriate selection of constraints type relations, including their level for each source, is an essential factor in the correct modelling of the tissue.

Table 1

Sources of uncertainty occurring in tissue modelling.

Source of uncertainty	Level, limitations	Type
Tissue properties	1000%–3000%	Epistemic/Aleatoric
Geometry shape	10%–50%	Aleatoric/Epistemic
Numerical errors	1%–5%	Aleatoric
Mathematical/physical model	undefined	Epistemic

Fig. 1. Uncertainty of data based on selected tissues.

2.2. Reliability problem

Apart from the issue of uncertainty, there is also the notion of reliability, and especially the reliability of the data constituting the parameters of the created model. Conductivity is an important parameter in the research on the influence of the electromagnetic field on tissues. It is the ability of a material to conduct an electric current. The electrical conductivity of the object, in turn, influences, for example, the ability to heat-up all or part of the area subjected to the field influence faster.

The parametric likelihood is illustrated in Fig. 1 (graph presented on this element was based on data obtained from [11–18]). This graph shows a significant range of variability for the conductivity parameter of selected seven tissues, distinguished especially in models used in brain simulations. Each point represents the actual conductivity value measured during both *in-vitro* (organs harvested) and *in-vivo* (patients during surgery). The visible points are a set read from eight selected scientific articles from among many others analysed during the research presented here. The articles were selected due to the legible form of biological parameters described in them, which were clearly characterized and described in those works, while the actual content is not relevant for this work.

The listed articles and sources, primarily medical, include parameters published in less than 25 recent years. This form of the presentation clearly outlines the possible discrepancy of the selected parameters, the measured values of which have changed and corrected over the years thanks to the general improvement of measurement accuracy and the development of testing methodology itself. It can also be easily read that the parametric discrepancy can even reach the level of hundreds of per cent between extreme values, especially in the case of those which were reliably collected in laboratory conditions.

2.3. Averaging problem

In the course of further research, the publicly available database of tissue parameters IT'IS [19] was also analysed. An additional element that was also considered as the source considered in the literature to be one of the most reliable in the field of tissue research − [14], in order to confirm the discrepancy which was previously observed.

As can be seen in Tables 2 and 3, the electrical parameter of conductivity was described as the mean and standard deviation of all available measurements, not as a single value. Such data presentation is a simplification, which may result in unfavourable calculation values. From the mathematical perspective, the concept of mean and deviation determines some freedom in a given range. It is usually a randomly selected value for computational systems from a full available range, using a defined (most likely Gaussian) distribution.

Table 2

Electrical parameters of biological tissues [19].

| Tissue con. [S/m]	avg	std. dev.	min	max
Skin	0.17	0.11	0.09	0.25
Bone	0.0035	0.00211	0.00185	0.00588
Muscle	0.36	0.2	0.02	0.67
Brain (Grey Matter)	0.24	0.11	0.11	0.48
Brain (White Matter)	0.27	0.38	0.06	1.2
CSF[a]	1.78	0.006	1.59	1.80
Blood	0.66	0.14	0.43	0.95

[a]Cerebrospinal fluid.

Table 3

Conductivity range of sample biological tissues [14].

Tissue	Conductivity range [S/m]
Muscle (X)	0.15 ± 0.01
Muscle (Y)	0.19 ± 0.018
Muscle (Z)	0.16 ± 0.037
Heart	0.48 ± 0.13
Skull	0.32 ± 0.38

Table 4

Conductivity parameters range of 9 patients during medical treatment [S/m] [20].

Tissue	P-1	P-2	P-3	P-4	P-5	P-6	P-7	P-8	P-9
GM	0.515	0.185	0.469	0.246	0.240	–	0.200	0.372	0.379
WM	0.277	0.216	–	0.307	–	0.210	–	0.302	–
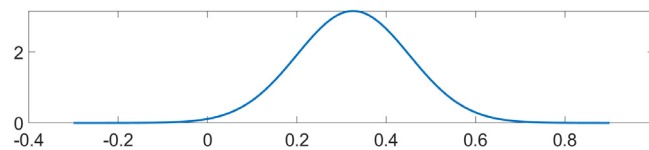
Fig. 2. Gaussian distribution of Grey Matter based on Table 4.

The Gaussian Distribution (also called the Normal Distribution) is characterized by the selection of *x* values from a specific interval according to Eq. (1)

$$f(x) = \frac{1}{\sigma\sqrt{2\pi}} e^{-\frac{1}{2}\left(\frac{x-\mu}{\sigma}\right)^2},$$ (1)

where μ is the mean (expected) value and σ is the standard deviation mentioned above.

The "unfavourable" values mentioned earlier can be observed by analysing the case presented in Table 4. The data collected represents the Grey Matter (GM) and White Matter (WM) conductivity values that were recorded during surgery for the nine patients. It is worth noting that the measurements were performed under the same conditions, with the same measuring tools, by the same medics team. Individual values are divergent from each other, which is confirmed by the fact that the parameter also varies among the patient population.

Taking such a small set of data as a reference point in tissue modelling, we can independently determine the mean and standard deviation parameters. Assuming that the set needs to provide close to 100% of the set of possible values, the deviation parameter should be designated as 3-Sigma. For the above set, the Grey Matter conductivity range will be the mean value $(\mu) = 0.3257$, and the deviation $(\sigma) = 0.3772$, respectively. For White Matter, mean $(\mu) = 0.2624$ and deviation $(\sigma) = 0.1397$.

Considering the generated Normal Distribution (Fig. 2), based on the previously calculated values, it can be observed that there are negative cases in the given range. This is an essential fact that using negative values from a biological point of view is not correct in the tissue modelling process. Also, looking from the analogous mechanical point of view − the conductivity parameter in the measurements identical to biological samples similarly assumes non-negative values. Thus, the direct translation of the collected values or measurements should consider the parameter value or the assumed set of values (represented by the implemented distribution).

In the case of the likelihood problem discussed in *Section* 2.2, which can be reduced by a sufficiently large measurement database, the averaging problem should be considered from the input data range representation side, e.g. parameters. Mathematically speaking, one should adopt such a distribution where values will not generate such problems and thus
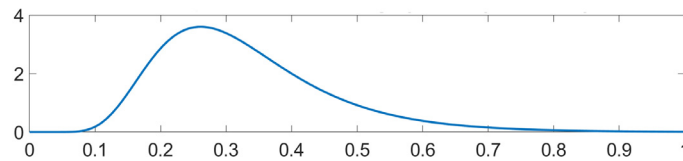
Fig. 3. Logarithmic-normal distribution based on Table 4.

Table 5
Assumptions of arm geometry model.

Parameter	Variability
Arm radius [cm]	4–5
Arm radius variability [%]	10
Arm skin thickness [cm]	0.2–0.4
Veins radius in X-axis [cm]	0.6–0.8
Veins radius in Y-axis [cm]	0.4–0.5

will not be negative ones. A possible example of such distribution, also used in the research presented here, is the Normal Logarithmic Distribution, defined by the equation Eq. (2).

$$f(x) = \frac{1}{x\sigma\sqrt{2\pi}} \exp\left(-\frac{(\ln x - \mu)^2}{2\sigma^2}\right),$$ (2)

where μ is the mean (expected) value and σ is the standard deviation.

Using this approach, presented random values of the conductivity parameter, which can be used in further calculations, are illustrated in Fig. 3. It can be clearly stated that there are no negative values here. Of course, this is one of many available solutions to the problem since many more statistical distributions describe a certain range of randomness in a given range. In the presented research, however, this particular approach was selected because of the good representation of the electrical parameters of tissues based on the data collected in the literature, with no negative values present. Moreover, this distribution is quite simple to implement in numerical calculations and follows the scheme of an effective methodology adopted in the course of experiments.

2.4. Geometry problem

In tissue modelling, an important element is the geometry of the examined object. The source of uncertainty, which is the geometry of the shape, mentioned in *Section* 2.1, accounts for the variability on the level of 10%–15%. This parameter can be influenced by biological and genetic conditions, age, diseases or the environment.

The mathematical models widely used in simulations are largely unchangeable. As in the examples discussed earlier, usually, one average form is used. In more complex simulations there may exist different models for genders or ones depending on age. In many cases, the source of these models is the publicly available VHP database (The Visible Human Project) [21] and its subsequent modifications. Since 2019 it is an open database of deceased female and male body slides, consisting of thin cross-sectional photos taken from magnetic resonance imaging, computed tomography and anatomical images.

Partial simulations, e.g. of a selected part of the body, usually use models based on simplified (from a geometry point of view) schematic tissue. In one of the previous studies performed by the authors, the arm cross-section model was used to simulate EMS, which included four selected tissues with the resulting model shown in Fig. 4. It included the outer skin (1), meat tissue (2), bone (3), and a venous complex (4). It should be clearly stated that this model is also structurally simplified, but research at this stage included the influence of geometry and biological parameters variability in the EMS simulation. Based on the IT'IS database and biological measurements of models from VHP scans, the features of geometry variability parameters were adopted according to the following assumptions (Table 5). The arm cross-section radius in the range of 4–5 centimetres was taken into account, with an additional value of the variation of 10%. The thickness of the skin layer was defined between 0.2 and 0.4 centimetres. Based on the cross-sectional model of the arm (see Fig. 4 on the left), the venous area was defined elliptically with the radius value independent for both axes.

3. Model creation

Encountered and existing problems related to the tissue representation discussed in *Section* 2 allowed for ordering a certain degree of correctness for the process of modelling, parameterization and defining a more realistic representation. Tissue modelling studies conducted in recent years also included the influence of external factors on the samples and thus on the measured electrical parameters. Given that the research focuses mainly on the concept of EMF, further considerations will continue on this path.
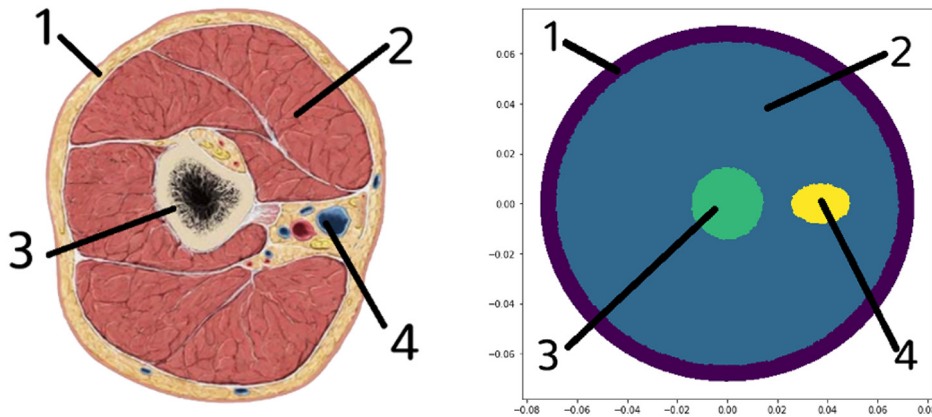
Fig. 4. Cross-section (left) [22] and simplified model (right) of human arm.

Table 6
SAR limits on mobile devices based on FCC/IEC.

Standard	Level [W/kg]	Volume mass [g]
US (FCC)	1.6	1
EU (IEC)	2	10

3.1. Standardization issue

It should be noted that there are no specific uniform simulation conditions for research conducted in the field of the discussed therapies or the impact of the field on the organism. Defined by global standards such as FCC (in the United States) or IEC (in Europe), the parametric conditions do not specify the concept of tissue variability or the variety of models to be simulated. They assume that the human is "averaged" and that the conditions imposed for the vast majority of the population are sufficient to give "confidence" that a given test, device, or procedure is safe.

An excellent example of a discrepancy in the subject matter discussed in this study, even in relation to generally accepted standards, is the Specific Absorption Rate concept (SAR). It is a measure of the rate at which the energy emitted by a device is absorbed by tissue (in this case, the human body) when it is exposed to radio waves. It is assumed to be the ratio of the power absorbed by the mass of tissue, and the unit is watt per kilogram $[\frac{W}{kg}]$ — as presented in Eq. (3).

$$SAR = \int_{sample} \frac{\sigma(\mathbf{r})|\mathbf{E}(\mathbf{r})|^2}{\rho(\mathbf{r})} \mathbf{r}, \tag{3}$$

where σ is the electrical conductivity of the sample [S], $\mathbf{E}$ is the RMS value of the electric field, and ρ is the sample density defined by the standard.

Table 6 shows the SAR values for US and European standards. Even while disregarding the conversion itself, the standards are incomparable to each other. The discrepancy also affects the possibility of adopting a given standard as a pattern.

Considering the example of the cross-section of the arm in the appropriate scale (in Section 2.4), applying both standards apart will also ensure independent results without the possibility to simply refer them to each other. This results in a situation when a potentially safe device that complies with the FCC standard may not comply with the IEC standard or vice versa. Therefore, when preparing the scenario for such calculations, the standardization and legal issues should also be taken into account.

3.2. Simulation assumptions

Preparing a model of a selected tissue (or a set of tissues) and determining their parameters is one of the necessary steps before the topic of simulation is even considered. The single static model in a single simulation is not a good source of the result since it relates to one specific case. In order for the results to be reliable, a certain scale is required for all operations.

Nowadays, many specialized programs are available that can perform calculations in dedicated environmental conditions for specific scenarios, taking into account almost any variation scale. Technological development has also shown the possibility of using more efficient resources, such as GPU (Graphic Processing Unit) cards, HPC (High-Throughput Computing) cluster solutions or Cloud Computing. Such solutions can achieve more accurate results in a much shorter
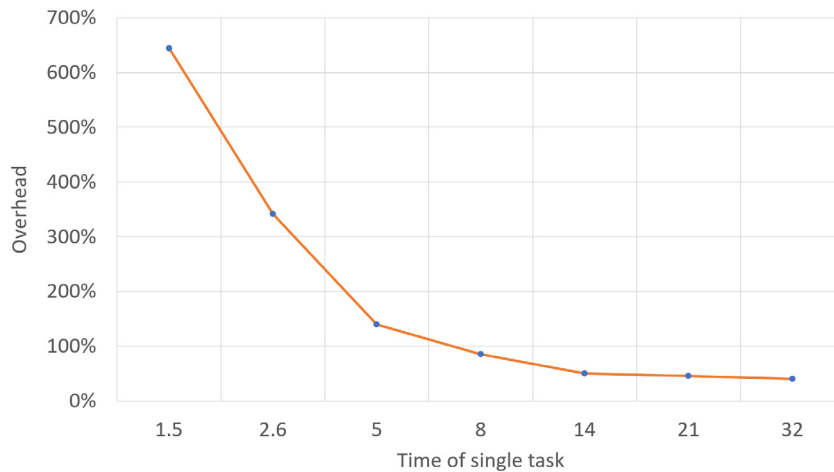
Fig. 5. Total overhead related to time of single simulation (task) [7].

time. It becomes obvious that the time is shortened, but the accuracy of the results depends on all factors together — used model, selected parameters, the adopted methodology and the calculation unit used.

In recent years, studies have managed to develop a procedure for dealing with such complex problems as tissues. The electromagnetic field environment is only one of the many available, as are the mathematical descriptions used as conditions for such simulations. This paper assumes the adoption of a more complex and faithful object methodology as well as multi-variable handling in order to ensure more accurate calculation results.

It is worth mentioning here the key coefficient in the case of computer simulation, which is an often-overlooked parameter — the Overhead. Conventionally it can be defined as shown in Eq. (4).

$$Overhead = \frac{Time_{(Total)}}{Time_{(Comp)}} - 1, \tag{4}$$

where $Time_{(Total)}$ is the total work time of the compute unit and $Time_{(Comp)}$ is the actual computation time.

It is an arbitrary value of computer working time, which is not strictly computing time. Ideally, the simulation should start and end at a precise start–stop time. In reality, however, before the actual simulation of the assumed computational conditions can take place, the computational unit needs to load libraries, define the memory area and copy the source data so that the actual computation can start. A similar situation happens when the calculations are completed — data must be saved in the appropriate memory area, transferred to the destination, and the available resources released for the needs of other processes in the system. In general, as can be seen in Fig. 5, the more time-consuming the task is, the less time during the actual computations will be spent on the side tasks.

The above situation is one of the reasons why the precise model and carefully selected, complex calculation conditions are such important factors in research performed in this work. Extending the computation time ensures the optimal use of resources in the global perspective of computer working time. At the same time, many independent calculations can be performed, which will only ultimately increase the reliability of the final result.

4. Simulation process

Based on the problems considered and analysed in the previous *Sections* as well as the adopted methods, a scenario was prepared that collected the discussed aspects and problems related to tissue representation for the preparation of a computational model. One example of this is a medical problem defined as a phenomenon of controlled, selective energy transfer known as "Magnetic Fluid Hyperthermia Therapy" (MFH) [23]. The problem concerns the creation of thermal conditions in an optimal place, which will support oncological treatment. For the MFH model described in the article, an implant is additionally used, which, when activated in the right place, is able to function according to the medical plan (Fig. 6).

Considering such a problem, optimizing the position of the system in such a way that the used implant will work most effectively becomes very important since it can increase the effectiveness of the entire therapy. The visualization of the electromagnetic field for Pancake Coils is shown in Fig. 7.

4.1. Physical definition

In order for the system to fulfil its task, it is necessary for the simulation to include not only the modelled object (affected by the field), but also the position of the coils. The distribution of the magnetic field for the coils in the real
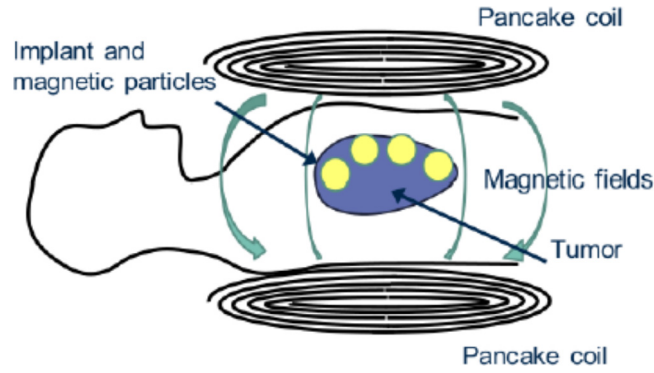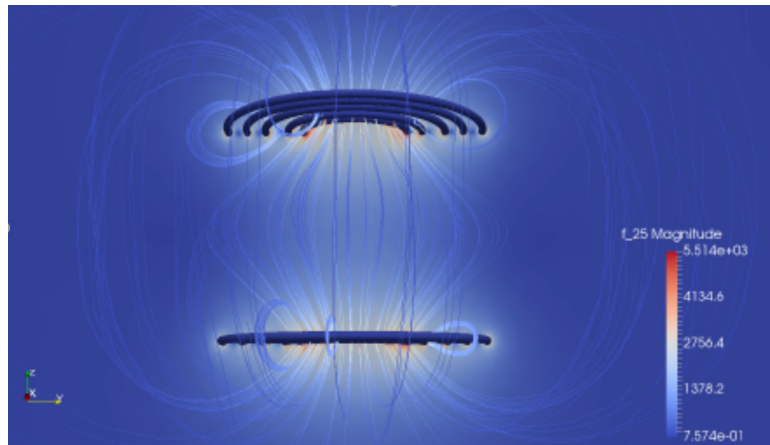
Fig. 6. MFH model based on [23].

Fig. 7. Pancake coil magnetic field transmission.

scale is realized directly from Ampere's law, defined here as the differential presented in Eq. (5),

$$\nabla \times \vec{H} = \vec{J},$$ (5)

where ∇ is the rotation operator $[\frac{1}{m}]$, $\vec{H}$ is the strength of the magnetic field $[\frac{A}{m}]$ and $\vec{J}$ is the density of the current flowing through the element $[\frac{A}{m^2}]$.

Using the Coulomb Gauge Index as presented in Eq. (6),

$$\nabla \cdot \vec{A} = 0,$$ (6)

where $\vec{A}$ is a magnetic vector potential $[\frac{V \cdot s}{m^{-1}}]$, in turn knowing that rotation $\vec{A}$ is equal to the value presented in Eq. (7),

$$\vec{B} = \nabla \times \vec{A}$$ (7)

where $\vec{B}$ is magnetic flux density $[T]$.

Then relationship with the magnetic field strength vector $\vec{H}$ can be defined as presented in Eq. (8)

$$\vec{B} = \mu \times \vec{H}$$ (8)

where μ is the magnetic permeability of the medium $[\frac{H}{m}]$, which in turn can unambiguously lead to the form presented in Eqs. (9) and (10).

$$-\frac{1}{\mu}\nabla^2 \mathbf{H} = \mathbf{J},$$ (9)

$$\mathbf{B} = \nabla \times \mathbf{A},$$ (10)

From the mathematical perspective, the computational problem presented in this way allows for the correct modelling of the field distribution for the system in the pancake coils formation in the test scenario.

4.2. Model implementation

The model discussed above was described using the Python language, and the FEniCS [24] software. The electrodes around the object are defined in the form of dots with a certain diameter distributed in space (representing the coils). They were taken at an appropriate distance from the simplified object located in the field created by the coils.

The simulation scenario included the variable arrangement of the coils in the *Y*-axis position at the same height. The aim was to ensure the simultaneous optimization of the simulation results for finding the solution. The points were placed randomly in the designated interval by the function *uniform* between *r_range* and *z_range*. Used method is outlined in Listing 1.

Listing 1: Defining position of the coils and boundary conditions.

```
#generate coil wires in space
r_range = (MIN, MAX)
z_range = (MIN, MAX)
c1 = Point( uniform(r_range[0], r_range[1]), uniform(z_range[0], z_range[1]) ), ...,
c5 = Point( uniform(r_range[0], r_range[1]), uniform(z_range[0], z_range[1]) )
```

The next step was defining the objects and generating the model mesh based on standard procedures used in the FEniCS program, as presented in Listing 2.

Listing 2: Object definition and model mesh generation

```
# Set subdomains for wires
domain.set_subdomain(1, cable)
domain.set_subdomain(2, body)

# Create mesh
mesh = generate_mesh(domain, 100)

# Define function space
V = FunctionSpace(mesh, 'CG', 1)
```

In the next step, the "body" object in the form of a simplified rectangle was defined. The detailed model was intentionally not implemented in this simulation because the assumptions included the appropriate selection of the optimization algorithm and verification of the computational effects for the therapy. The whole model has been symmetrically cut off in relation to the *Z*-axis due to the applied cylindrical coordinate system of the coils, according to Eq. (11). Next, the model mesh and Dirichlet boundary conditions were parameterized, as shown in Listing 3.

$$-\frac{1}{\mu}(\nabla^2 \mathbf{A}_\varphi - \frac{\mathbf{A}_\varphi}{r^2}) = \mathbf{J}_\varphi,$$
$$\mathbf{B} = [-\frac{\partial A_\varphi}{\partial z}, \frac{A_\varphi}{r} + \frac{\partial A_\varphi}{\partial r}], \tag{11}$$

Listing 3: Parameterization of model mesh and Dirichlet boundary conditions

```
# Define boundary condition
bc = DirichletBC(V, Constant(0), 'on_boundary')

# Define subdomain markers and integration measure
markers = MeshFunction('size_t', mesh, 2, mesh.domains())
dx = Measure('dx', domain=mesh, subdomain_data=markers)

# Current density (magnitude) [A/m^2]
Jv = 100/(DOLFIN_PI*0.005*0.005)
J_N = Constant(Jv)

mu = Constant(4*pi*1e 7)

# Define variational problem
A_phi = TrialFunction(V)
v = TestFunction(V)
r = Expression('x[0]', degree=1)
a = (1/mu)*(dot(grad(A_phi), grad(v)) + A_phi*v.dx(0)/r)*dx
L = J_N*v*dx(1)
```

For the model defined in this way, the simulation output parameters were chosen, which required the determination of energy values in the body for a given solution. The method used for this part is presented in Listing 4.

Listing 4: Calculating energy in a "body" from a simulated magnetic field.

```
#compute magnetic field
B = project(as_vector(( A_phi.dx(1), (A_phi/r + A_phi.dx(0)))), W)
H = project(B/mu,W)

#print calculated energy in body
body_ener = assemble( 2*DOLFIN_PI*r*inner(B,H)/2*dx(2) )
```

The final results of the simulation were saved as the energy value and the position of the coils for this simulation — respectively x and y for the defined $\{c1...c5\}$. The example results of this operation are shown in Listing 5.

Listing 5: Example results for single simulation

```
0.000381497978835 0.194462546647 0.158087010577 0.0932727256494 0.224560813522 0.106482653009 0.277131816951
    0.139521639277 0.20530100616 0.247650543411 0.29650088867
```

The values indicated respectively the maximum value of the energy stored in the system and the position of the centres for the five consecutive coils in the *XY* system.

4.3. Simulation

The adopted scenario included the methodology of repeatedly running a single simulation for random variables in a given range. This approach, called the Monte Carlo method (or often "brute-force"), is an inefficient, prolonged solution. However, it allows for more optimal use of computer platforms and, more precisely, distributed systems that were used and the main environment during the research.

The computing platform was a distributed structure based on the Microsoft Azure platform [25] with a dedicated management system for scientific purposes HTCondor [26]. The configuration was prepared according to the proprietary model scheme (as presented in Fig. 8), which proved successful in the experiments carried out in the tasks referred to as "High Compute".

The "Hight Computer term is widely used in IT [27] and science [28], as a definition covering all high-performance systems, large-scale systems and data computing systems referred to as "Big Data" for both scientific and commercial purposes [29,30].

The MS Azure Cloud Computing Environment treats the Resource Group as the main work object, i.e. a dedicated place in the server room from which resources can be used according to the needs under the conditions specified by the subscription. The computing system consisted of networks of the following virtual machines:

- 1× central management unit (Central Manager) — handling commands for starting machines, transferring tasks and receiving results from worker nodes,
- 1000× computing machines (Worker) — receiving tasks from the managing unit, performing computational tasks and returning results.

4.4. Optimization results

The adopted methodology assumed the logical substitution of the position of the coils in a given system in 100,000 independent simulations. Due to the scale, the model was implemented on two levels:

- 1D layout — the arrangement of the coils in one plane, with a variable radius, keeping a constant distance from the object,
- 2D layout — the arrangement of the coils in two planes, with a variable radius, maintaining a variable distance from the object.

Both systems were corrected in relation to each other, remembering the maximum energy value and the position of the coils in relation to all the results obtained at the current stage of calculations. The best results for each method are shown in Fig. 9. On the left, there is a 2D system visualized; on the right, the 1D system and the positioning of the coils in space, which provide the best solution (energy value) for the most effective therapy — according to the adopted scenario.

From the computational point of view, it could be concluded that after three hours of computing on a cluster of 1000 virtual machines, the method is slowly converging (Fig. 10). However, it can be assumed that the computational scale gave very detailed results in a given time interval.
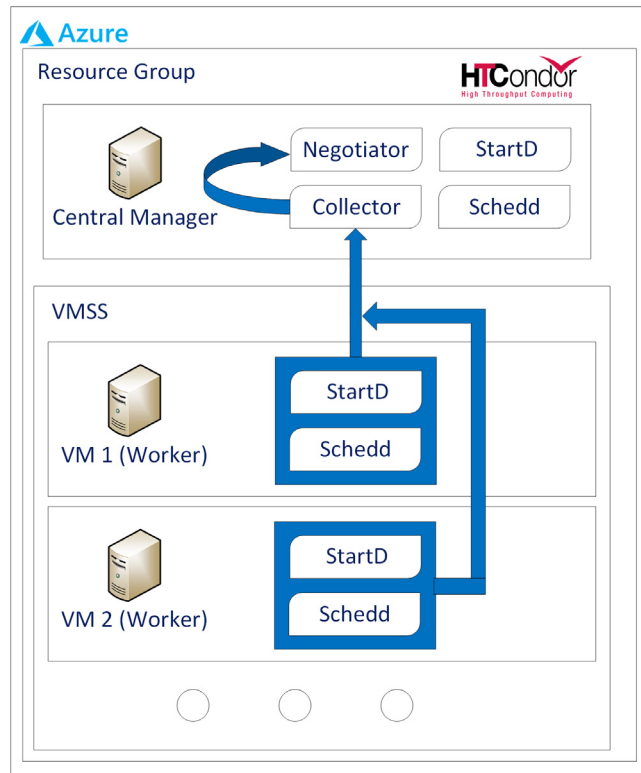
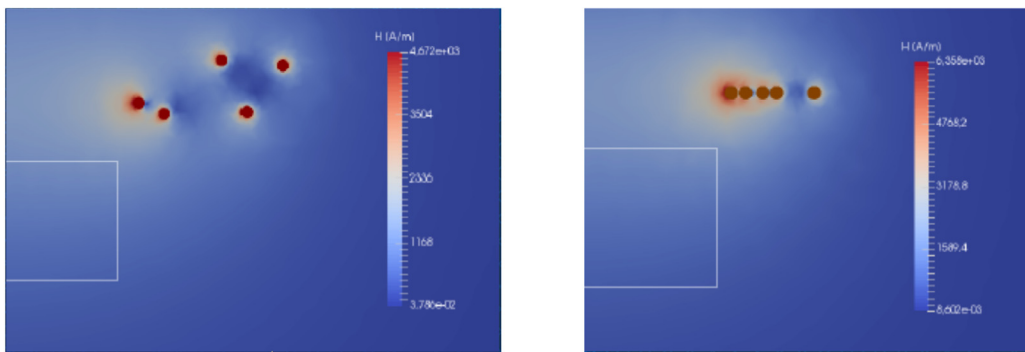**Fig. 8.** Computing platform structure used in coil simulation.

Fig. 9. "Brute force" coil optimization in 1D (left) and 2D (right) systems.

5. Conclusions

In the course of the research conducted in recent years (the results of which have been presented here), methodologies for the modelling of biological objects (tissues) in bioelectromagnetic problems have been developed. The problem of computer imaging of tissues is highly complex, and it is not possible to accurately reproduce them on a micro-scale. Treatment of tissues "molecularly" is almost impossible or involves much computational effort.

Determining the relationship between such a precisely mapped model mesh, taking into account the concept of the variability, the existing environment, building a mathematical model or uncertainty, is currently beyond the computational capabilities of even supercomputers. Additionally, the issue of detail and scale of the problem should be considered for each such application.

It is the given fact that increasing accuracy of the model will result in similar relations in the obtained results, which may include previously unaccounted cases and threats, e.g. for humans — whether in therapy or in an electronic device that a human will have to deal with. At the same time, it will result in increasing computation time and problems with preparing actually executable scenarios.
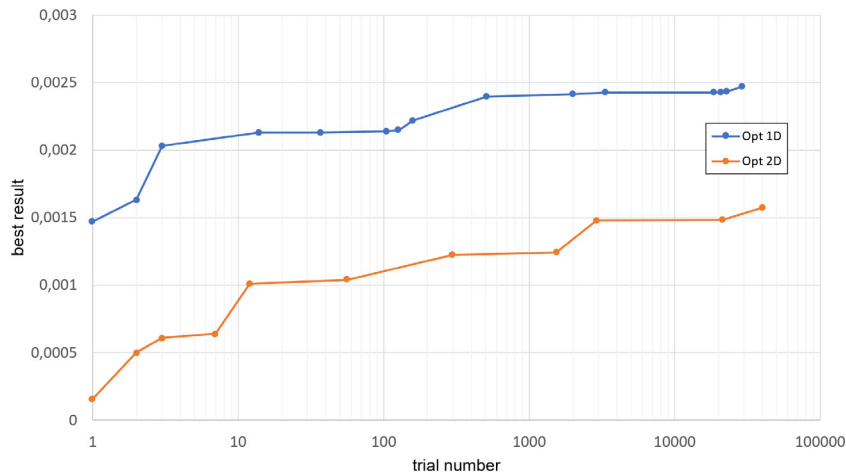
Fig. 10. Convergence of optimization process in 1D and 2D systems.

The discussed research includes, first of all, a solid research review related to the aspects of tissue modelling with the use of computing in simulations. The size of the problem forced a large-scale view of the issue, covering both physical and mathematical parametric issues.

The article summarizes the recent years of research aimed at using the technological and engineering possibilities available today in research problems related to tissues. Individual research and conducted arguments were extended by a methodical approach to the problem and a collective summary with a description of the impact of each factor on the simulation process, the accuracy achieved and the reliability of the obtained input information.

The problems related to the tissue representation collected in this work are primarily used to show possible room for improvement in the case of factors with a significant impact on calculations reliability. Not all of the issues raised may be right, just as not every parameter should be so detailed. However, the key is to recognize the problem and use the available computing resources to the maximum extent. This will allow for the natural development of science and verify the discussed sources of uncertainty and the presented scale.

Acknowledgements

References

[1] R. Jr, D. Daniel, D.F. Bruley, M.H. Knisely, A digital simulation of transient oxygen transport in capillary tissue systems (cerebral grey matter). Development of a numerical method for solution of transport equations describing coupled convection diffusion systems., AIChE J. 15 (6) (1969) 916–925, http://dx.doi.org/10.1002/aic.690150620.

[2] P.L. Gould, A. Cataloglu, R.E. Clark, Mathematical modelling of human aortic valve leaflets, Appl. Math. Model. 1 (1) (1976) 33–36.

[3] G.C.-C. Lo, Estimation of Epicardial Electrical Potentials from Body Surface Measurements Based on a Digital Simulation of the Human Theory (Ph.D. thesis), Imperial College London, 1977.

[4] V. Libertiaux, F. Pascon, Differential versus integral formulation of fractional hyperviscoelastic constitutive laws for brain tissue modelling, J. Comput. Appl. Math. 234 (7) (2010) 2029–2035.

[5] N. Mangado, G. Piella, J. Noailly, J. Pons-Prats, M.Á.G. Ballester, Analysis of uncertainty and variability in finite element computational models for biomedical engineering: characterization and propagation, Front. Bioeng. Biotechnol. 4 (2016) 85.

[6] A. Krupa, B. Sawicki, Measurement-based stochastic models of biological materials, in: 18th International Conference Computational Problems of Electrical Engineering (CPEE), 2017, pp. 1–4, http://dx.doi.org/10.1109/CPEE.2017.8093068.

[7] B. Sawicki, A. Krupa, Optimization of coil geometry using Monte Carlo method with htcondor and microsoft azure technologies, Prz. Elektrotech. 95 (5) (2019) 114–118, http://dx.doi.org/10.15999/48.2019.05.28.

[8] B. Sawicki, A. Krupa, Study of biological tissues variability modeling, in: 16th International Conference on Computational Problems of Electrical Engineering (CPEE), 2015, pp. 174–176, http://dx.doi.org/10.1109/CPEE.2015.7333368.

[9] B. Sawicki, A. Krupa, Experiments with models of variability for biological tissues, Prz. Elektrotech. 92 (7) (2016) 83–86, http://dx.doi.org/10.15199/48.2016.07.18.

[10] A. Krupa, B. Sawicki, Preliminary study of random variable algebra for biological tissue description, in: 17th International Conference Computational Problems of Electrical Engineering (CPEE), 2016, pp. 1–55, http://dx.doi.org/10.1109/CPEE.2016.7738732.

[11] J. Haueisen, C. Ramon, M. Eiselt, H. Brauer, H. Nowak, Influence of tissue resistivities on neuromagnetic fields and electric potentials studied with a finite element model of the head, IEEE Trans. Biomed. Eng. 44 (8) (1997) 727–735.

[12] G. Schmid, G. Neubauer, P. Mazal, Dielectric properties of the human brain measured less than 10 hours post mortem, in: Proceedings of the General Assembly of the International Union of Radio Science, Citeseer, 2002, pp. 1759–1762.

[13] C.H. Wolters, A. Anwander, X. Tricoche, D. Weinstein, M.A. Koch, R.S. Macleod, Influence of tissue conductivity anisotropy on EEG/MEG field and return current computation in a realistic head model: a simulation and visualization study using high-resolution finite element modeling, NeuroImage 30 (3) (2006) 813–826.

[14] C. Gabriel, A. Peyman, E.H. Grant, Electrical conductivity of tissue at frequencies below 1 MHz, Phys. Med. Biol. 54 (16) (2009) 4863.

[15] T. Jochmann, D. Güllmar, J. Haueisen, J.R. Reichenbach, Influence of tissue conductivity changes on the EEG signal in the human brain–a simulation study, Z. Med. Phys. 21 (2) (2011) 102–112.

[16] A. Khaleghi, M.E. Sendi, R. Chavez-Santiago, F. Mesiti, I. Balasingham, Exposure of the human brain to an electromagnetic plane wave in the 100–1000 MHz frequency range for potential treatment of neurodegenerative diseases, IET Microw. Antennas Propag. 6 (14) (2012) 1565–1572.

[17] M. Fernández-Corazza, L. Beltrachini, N. Von Ellenrieder, C.H. Muravchik, Analysis of parametric estimation of head tissue conductivities using electrical impedance tomography, Biomed. Signal Process. Control 8 (6) (2013) 830–837.

[18] P.C. Miranda, A. Mekonnen, R. Salvador, P.J. Basser, Predicting the electric field distribution in the brain for the treatment of glioblastoma, Phys. Med. Biol. 59 (15) (2014) 4137.

[19] IT'IS Database, 2010, (2010 (accessed September 1, 2020). URL https://itis.swiss/.

[20] J. Latikka, T. Kuurne, H. Eskola, Conductivity of living intracranial tissues, Phys. Med. Biol. 46 (6) (2001) 1611.

[21] The national library of medicine's visible human project, 2020, (1986-present (accessed September 1, 2020)). https://www.nlm.nih.gov/research/visible/visible_human.html.

[22] E.M. Abdullzaher, Biceps brachii - Physiopedia, 2017, (2017 (accessed September 1, 2020)). URL https://www.physio-pedia.com/Biceps_brachii.

[23] S. Yamada, Y. Ikehata, T. Ueno, H. Nagae, Wireless power transfer system for hyperthermia therapy, in: Proceedings of the 2nd Frontiers in Biomedical Devices Conference, Vol. 111, Citeseer, 2007, p. 112.

[24] FeninCS Project, 2020, (2003-present (accessed September 1, 2020)). URL https://fenicsproject.org/.

[25] Microsoft Azure, 2020, (2020 (accessed September 1, 2020)). URL https://azure.microsoft.com/.

[26] High throughput computing, 1988, (1988-2020 (accessed September 1, 2020)). URL https://research.cs.wisc.edu/htcondor/.

[27] What is high-performance computing - answer from SUSE defines, 2020, (2020 (accessed September 1, 2020)). URL https://susedefines.suse.com/definition/high-performance-computing/.

[28] D. Miles, Compute intensity and the FFT, in: Proceedings of the 1993 ACM/IEEE Conference on Supercomputing, 1993, pp. 676–684.

[29] C.D. Patel, R. Sharma, C.E. Bash, A. Beitelmal, Thermal considerations in cooling large scale high compute density data centers, in: ITherm 2002. Eighth Intersociety Conference on Thermal and Thermomechanical Phenomena in Electronic Systems (Cat. No.02CH37258), 2002, pp. 767–776, http://dx.doi.org/10.1109/ITHERM.2002.1012532.

[30] J. Cho, T. Lim, B.S. Kim, Measurements and predictions of the air distribution systems in high compute density (internet) data centers, Energy Build. 41 (10) (2009) 1107–1115.